ADVANCED MATERIALS

Supporting Information

Oxide Resistive Memory with Functionalized Graphene as Built-in Selector Element

Yuchao Yang, Jihang Lee, Seunghyun Lee, Che-Hung Liu, Zhaohui Zhong, and Wei Lu*

Supporting Information

Oxide Resistive Memory with Functionalized Graphene as Built-in Selector Element

Yuchao Yang, Jihang Lee, Seunghyun Lee, Che-Hung Liu, Zhaohui Zhong, and Wei Lu*

The performance of Ta_2O_{5-x}/TaO_y bilayer devices with graphene electrodes is compared with that of devices based on metal electrodes. In contrast to the linear on-state characteristics of $Pd/Ta_2O_{5-x}/TaO_y/Pd$ devices (Refs. 25 and 26), the $MLG/Ta_2O_{5-x}/TaO_y/MLG$ devices show high on-state nonlinearity that is desirable for mitigating the sneak path problem, as shown in Figure 1e. The power consumption of the devices was estimated from the reset voltage and current, and it was found that after the replacement of metal electrodes with graphene electrodes the power consumption of the memory device is typically reduced from ~1.7 mW to ~0.4 mW. The main reason for the reduced power reduction is the more resistive graphene electrode which acts as a built-in series-resistor that reduces the programming current. Other performance metrics including retention (>1 hour), and endurance (>3000 W/E cycles, Fig. S1) can also be obtained in the still-optimized devices based on functionalized graphene electrodes. We expect that continued optimization of the devices will be able to improve the performance further.
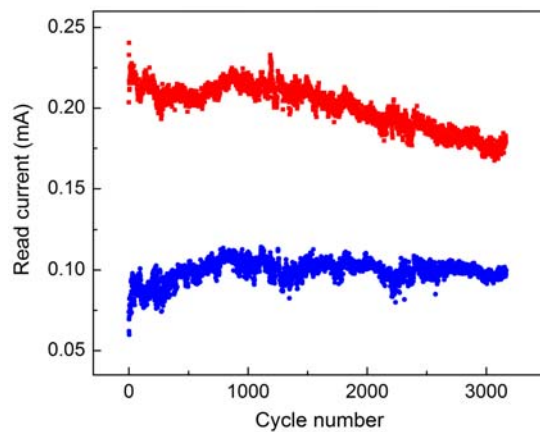
Figure S1. Endurance of MLG/Ta_2O_{5-x}/TaO_y/MLG device with a size of 100 μm.
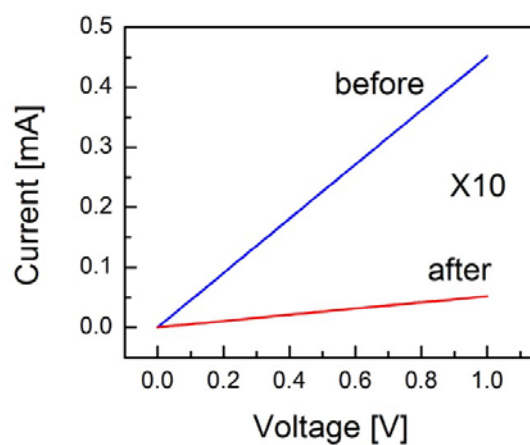

Figure S2. *I–V* characteristics of graphene bottom electrodes without any oxide deposition (before) and after the MLG/Ta_2O_{5-x}/TaO_y/MLG device fabrication process (after). The electrode resistance was found to increase by a factor of ~10, showing a resultant resistance of ~20 kΩ.
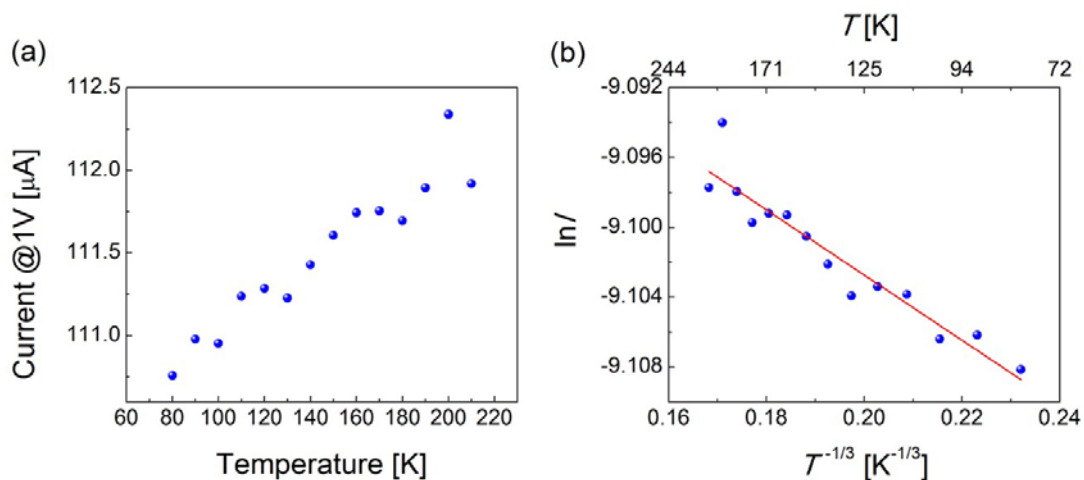
Figure S3. (a) *I–T* characteristics of the HRS state of the functionalized graphene BE (read at 1 V) measured from a different device, showing a monotonically increasing trend of current as temperature increases. (b) Fitting of the data in (a) with the VRH model. A linear relationship between ln *I* and $T^{-1/3}$ was revealed, indicating VRH as a plausible conduction mechanism in the partially oxidized graphene.
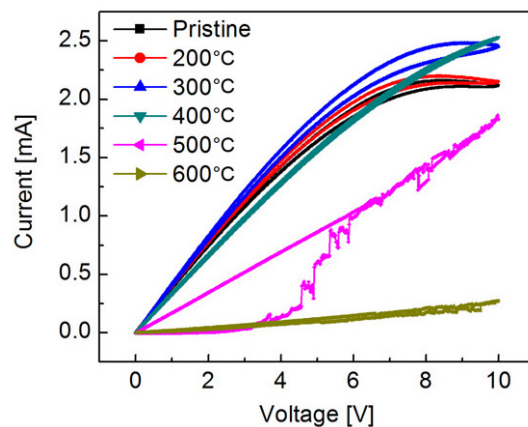
Figure S4. Control experiment showing *I–V* characteristics of graphene films at different annealing temperatures. The graphene devices were contacted with Pd pads instead of Au/Ti pads. Similar resistive switching behaviors can be observed after the oxidation of graphene.

Additional control experiments were carried out to verify the switching behavior in oxidized grapheen using Pd contacts instead of Au/Ti contacts, to exclude the possibility of forming a TiO_x layer during oxidization that may contribute to the observed switching behavior (e.g. Figure 5a). Figure S4 shows the *I-V* characteristics of graphene films contacted by Pd contacts (which also forms Ohmic contact with graphene). Similar behaviors as those in Figure 5a were reproduced, validating the switching behavior originated from controllably oxidization of graphene.